TN-52

OYO TECHNICAL NOTE

Measurment of S wave Velocity of the Ground
and
Application of S Wave Velocity Data
For Civil Engineering

by Shigekazu Uchiyama, Keiji Tonouchi and Tsuneo Imai

(Geotechnical Institute, OYO Corporation)

RP-4162 NOV 1984

GEOLOGICAL, GEOPHYSICAL AND GEOTECHNICAL SERVICE AND INSTRUMENTATION

OYO CORPORATION TOKYO JAPAN

• URAWA RESEARCH INSTITUTE •

2-19 DAITAKUBO 2 chome URAWA SAITAMA 336 JAPAN / TELEX : 02923-080 OYOJPN J

... KUDAN KITA 4 chome CHIYODA-KU TOKYO 102 JAPAN

Abstract

Site investigations for civil engineering and other purposes in Japan often include measurement of P and S wave velocities taken in a single bore-hole. This type of measurement is called PS logging in Japan.

In this paper, we describe two methods of PS logging that have been in general use, and one new method recently developed. In the traditional methods, the receiver is fixed within the boehole or set on the surface of the ground. In the new method, the receiver is not fixed, but is freely suspended in the borehole mud. From this characteristic, the new method is called "Suspension PS logging".

Next, we present some typical examples of messurement results obtained by three methods in soil, soft rock and hard rock formations. The records are good examples of elastic waveforms to depths of hundreds of meters.

Examples of applications of elastic wave velocity, with special reference to S wave velocity for engineering purposes are given. The first application of S wave velocity is calculation of ground motion that would result from an earthquake, information that is required in aseismic design. In recent years, we have been engaged in calculation of probable ground motion during earthquakes throughout certain prefectures for use by prefectural governments in planning disaster prevention programs. Surveys of this type are known as "microzonation surveys".

Another application of elastic wave velocity is to evaluate the dynamic properties of formations.

We have also been investigating the relationship between elastic wave velocity and other elastic coefficients obtained from other in situ or laboratory tests. We have found that elastic wave velocity, especially S wave velocity, has good correlations with these coefficients. From these correlations, certain key values of formations can be postulated.

By using waveform records obtained with PS logging, we are also trying to calculate Q-value (quality factor), which shows attenuation of elastic waves propagated through a formation. This value is very important for calculating ground motion. An example of calculation of Q values is presented along with a comparison of Q values obtained by PS logging and by other methods.

Preface

There are three methods for the investigation of the elastic wave velocity structure of formations. These are: (1) the refraction, (2) reflection and (3) logging methods.

In the refraction method, it is necessary to use a measuring line of a length at least 3 to 5 times that of the measuring depth. For this method to work, each layer must have progressively higher velocity values. The reflection method cannot be used by itself to determine elastic wave velocities of formations. In addition to the above difficulties with these two methods, it is very difficult to measure S wave velocity values of formations by either of these two methods. However, the logging methods can be easily used to direct measurement of real velocity values.

Measurement of velocity of P waves, which is one kind of elastic wave, has long been carried out in borehole investigations in Japan at dam sites, etc. These measurement results are used to assess rock characteristics. However, such important data as shear modulus, Young's modulus, bulk modulus, and Poisson's ratio cannot be obtained from P wave velocity alone.

Attempts to measure S wave velocity began in the early 1960's in Japan. One result of this work is the Borehole Pick, which is an instrument that can be fixed to the borehole wall at desired depths. By the last half of the 1960's this instrument was being put to practical use measuring P and S wave velocities in boreholes. In Japan, the technique for measuring P and S wave velocities of formations is called "PS logging".

At present, PS logging is widely used for in situ investigations. The results thus obtained are used to calculate probable ground motion during earthquakes and to assess formation characteristics.

In recent years, a joint project between Mr. Kimio Ogura, of OYO Corporation, and Dr. Kitsunezaki has resulted in the development of a new type of instrument for PS logging, based on a new principle. This technique is called "suspension PS logging". This technique measures the velocity of elastic waves progated along the borehole wall. It uses a probe containing both seismic source and seismic receivers, a point in common with acoustic logging. However, the principles of wave generation and reception differ greatly between suspension PS logging and acoustic logging. We are presently engaged in compiling measurement data using this method.

We have also conducted investigations on the relationship between elastic wave velocity and several characteristics that express characteristic of formations or samples. These investigations make use of a large amount of data obtained from PS logging and other types of both in situ and laboratory tests. It was found that elastic wave velocity, in particular S wave velocity, shows good correlations with several coefficients. This implies that these coefficients can be used to infer a great deal of information about the ground that is essential in civil engineering and other fields.

We are also engaged in trying to calculate quality factor (Q value), which expresses the attenuation characteristics of formations, from PS logging waveform records. One interesting result of this research we have found is that Q values for soft layers are not necessarily smaller than for hard layers.

In the following sections, the above research is explained in detail.

Method of Measurement

In this section, we describe three kinds of PS logging methods. The first two methods have been in general use for a long time. The other is a new method, developed in recent years.

Figure 1 is a schematic diagram of the PS logging method. The Borehole Pick consists of three geophones (one for measurement of vertical and two for measurement of horizontal vibrations), a hydrophone and an azimuth detector. The Borehole Pick is encased in an inflatable rubber tube. By inflating this tube, the instrument is fixed against the borehole wall at the desired depth. Either gas or water is used to inflate the tube. A curved steel plate fitted over the rubber tube insures a firm fit against the borehole wall. As shown in Figure 1, P and S waves are generated on the surface of the ground. These are propagated through the formation and are detected as electrical signals by the Borehole Pick. These signals are amplified and recorded.

Vertical striking of the ground, either by ground hammering or weight dropping, is usually used to generate P waves. For measurement at greater depths, blasting is used instead of these methods to produce P waves of sufficient amplitude to reach the desired depth.

The wooden plank hammering method is used to produce S waves. First, the surface of the ground is leveled. A wooden plank is laid on the ground and a heavy weight is placed on one end. The edges of the plank are then struck with a sledgehammer to produce SH waves.

In actual measurement, measuring intervals are usually 2 meters. Measurement is carried out at each interval from the bottom to the top of the borehole. Figure 2 shows an example of waveform records obtained by PS logging. In the record, it can be seen that the S waveform records are the reverse of one another when the plank is struck from opposite sides. This characteristic of phase reversal is the key to identify S waves.

Figure 3 is a schematic diagram of another method of PS logging. In this method, blasting is conducted in the borehole and the resulting elastic waves are received at several points on the surface. This method is used when logging is conducted in sea or river bottoms, making surface wave generation methods impossible, or when borehole conditions are such that it is impossible to raise or lower a probe. When a blast is set off in a borehole, P and SV waves are generated. In this case, SV waves are most strongly pronounced diagonally in relation to the borehole axis; SV waves are not generated along the borehole axis and at right angles to it. Maximum amplitude of the waves differs with blasting depth and location of observation points on the surface. It is therefore necessary to establish several observation points located sufficiently far from the borehole at appropriate places on the surface. In Figure 3, there are 3 observation points. Three geophones, one for measurement of vertical vibrations and two for measurement of horizontal vibrations, were set at each of these points. Figure 4 shows an example of waveform records obtained by this method. Both P and S waves can be easily identified in these records. Figure 5 is a schematic diagram of the new suspension PS logging method. In this method, P waves and S waves are produced by sudden changes in pressure of the borehole mud. These pressure changes are effected by the horizontal motion of a rigid body in the borehole mud as it is struck by an electromagnetic hammer. The sudden pressure change causes displacement of the borehole wall. This displacement is then transmitted along the entire length of the borehole. The resulting movement of the borehole mud corresponds to borehole wall displacement, so detection of borehole mud movement is the same as detection of borehole wall displacement. The receiver used in this system has a specific gravity nearly equal to 1.0 in borehole mud. Because the seismic waves produced by this system are sufficiently longer than the diameter of the borehole, they may be considered to originate from a single point source in an infinite medium. Therefore, predominant S waves are produced in addition to P waves. Acoustic logging cannot detect S waves in formations having velocities lower than that of borehole mud. This is because in such low velocity layers, there is no critical angle of wave refraction. However, suspension PS logging can detect S waves in any formation regardless of velocity value, because S waves are directly produced by an electromagnetic hammer.

Figure 6 shows an example of waveform records obtained by this method. Spacing between the receivers is usually one meter. Both P and S waves can be easily identified in these records.

Some Examples of Measurement Results

Since the latter 1960s, we have conducted many site investigations using PS logging, which has yielded a large volume of measurement results.

Some examples of measurement results are shown in Figures 7 through 10. Each elastic modulus in these figures was calculated using P and S wave velocities and formation density values. The latter were obtained either by density logging or sample testing. In these figures, the S waveformn records were obtained by hammering the plank on one side only to avoid complication of waveforms.

Figure 7 shows information received in a layer consisting mainly of sand and silt. P wave velocity shows a remarkably abrupt change in P wave velocity at around 10 m. From this depth, the ground is saturated, while above 10 m, lower P wave velocities are obtained because the formation is unsaturated. In the saturated part of the formation, P wave velocity is about 1.6 km/s, which is close to that of P wave velocity in water.

Figure 8 shows measurement results from a soft rock formation mainly composed of sandstone, tuff and tuff breccia. Both P and S wave velocity value distribution shows the formation to be divided into 5 or 6 layers. P wave velocity values range from 1.59 km/s to 2.38 km/s. For S wave velocities, the range is from 0.48 km/sec to 1.0 km/s. Both P and S wave velocities increase gradually with depth. It may be assumed that in soft rock formations of sediment, etc., increasing overburden pressure results in increases in elastic wave velocities.

Figure 9 shows an example of measurement results from a hard rock formation. This formation consists mainly of diorite and diabase. Both P and S wave velocity distribution show a 3 layer structure of the ground. In the first layer, P wave velocity was 4.50 km/s and S wave velocity was 2.34 km/s. In the second layer, P wave velocity was 5.25 km/s and S wave velocity was 2.70 km/s. In the third layer, P waves were 6.20 km/s and S waves were 3.10 km/sec. The latter are very high values. This is the sole PS logging measurement result giving 6 km/s P waves and 3 km/s S waves.

Figure 10 shows results obtained by suspension PS logging. These results were obtained from the same site as shown in Figure 8. Comparing the two figures, we see that, whereas PS logging shows only a few velocity layers, suspension PS logging provides more detail on different velocities present in the formation. In this way, suspension PS logging is a useful method when it is necessary to obtained detailed velocity data in formations, such as when evaluating the characteristics of a formation composed of many thin layers.

Applications of S Wave Velocity

In Japan, S wave velocity values are applied to problems in earthquake engineering, architecture and civil engineering. The most important and direct application is for calculation of ground motion that would occur during an earthquake. This is done by analyzing seismic waves incident to the base layer and their transfer characteristics in the formation above the base layer. Ground motion $O(\omega)$ at the surface in a frequency domain can be expressed with the following equation:

$$O(\omega) = S(\omega) \cdot B(\omega) \tag{1}$$

where, $S(\omega)$ is Fourier spectrum of the incident seismic wave at the base layer and $B(\omega)$ is the Fourier spectrum of the transfer characteristics of the formation above the basic layer. The following equation expresses $B(\omega)$ when the S wave is vertically incident to the base layer.

$$B(\omega) = \frac{2i \cdot \rho n \cdot Vsn \cdot \omega}{B_{21} + i \cdot B_{11} \cdot \rho n \cdot Vsn\ \omega} \tag{2}$$

where, ρ_n is density at base layer and Vsn is S wave velocity, with no account taken of attenuation. Using Q value, the relationship between Vsn^* and measured S wave velocity Vsn is expressed as follows:

$$Vsn = Vsn^* \left(1 + \frac{i}{2Q}\right) \tag{3}$$

Also, B_{21} and B_{11} can be expressed with the product of the matrices of each layer above the basic layer:

$$B = \begin{vmatrix} B_{11} & B_{12} \\ B_{21} & B_{22} \end{vmatrix} = a_1,\ a_2,\ a_3 \cdots\ a_{n-1} \tag{4}$$

where, matrix ai of each layer can be expressed as follows:

$$ai = \begin{vmatrix} \cos\frac{\omega \cdot di}{Vsi} & \frac{1}{\rho i \cdot Vsi\ \omega} \cdot \sin\frac{\omega \cdot di}{Vsi} \\ -\rho i\ Vsi \cdot \sin\frac{\omega \cdot di}{Vsi} & \cos\frac{\omega \cdot di}{Vsi} \end{vmatrix} \tag{5}$$

Where, suffix i indicates the layer number from the surface layer toward the basic layer, di is the thickness of the layer and ρ_i, Vsi^* are the same quantity at each of the layers as described above.

Incident seismic waves $S(\omega)$ occurring at the base layer are represented by seismic waveforms selected from existing records taken during actual earthquakes. Selection is made on the basis of similarity of ground characteristics, frequency of earthquake occurrence and distance from earthquake prone locations. An example of calculation results is shown in Figure 11. This example is calculated for several points under different geological conditions with the same incident seismic wave. Variations in ground motion at the surface is largely due to geological conditions.

Subsurface ground motion can be calculated by the same method. Figure 12 gives an example of this type of calculation. In this figure, acceleration and shear stress in the ground are calculated. When probable shear stress produced in the ground by an earthquake is calculated, this can be used to estimate the probability of liquefaction. In recent years, some prefectures in Japan have sponsored surveys using such calculations to estimate probable ground motion during a major earthquake throughout the prefectures. These results are then used in planning earthquake countermeasure programs. Figure 13 shows an example of the kind of calculation involved in these surveys. The prefecture was divided into a grid, each mesh of which measured approximately 1.1 Km x 0.9 Km. Using an empirically derived equation, peak acceleration at the base rock for each mesh was computed. Using this data and amplification of overburden layer, surface acceleration during an earthquake was then estimated for each mesh. Finally, we expressed these results in the form of seismic intensity maps. Because it is not practicable to conduct PS logging over the vast area of an entire prefecture, S wave velocity values are commonly estimated, using the relationship between S wave velocity and N value, obtained by the standard penetration test. This relationship is described below.

In structural design, it is necessary to know such characteristics of the ground as deformation and strength values. The general procedure for obtaining these values has been borehole deformation testing. However, the design of major structures calls for measurement depths of hundreds of meters. At such depths, it is economically unfeasible to carry out deformation testing continuously from the bottom to the top of the borehole. Instead, borehole measurements of elastic wave velocity (S wave velocity in particular) have been used to indirectly estimate the strength and deformation characteristics of the ground. Figure 14 shows an example of estimation of formation characteristics according to this method. In addition to elastic wave velocity, the figure shows deformation coefficient (elastic modulus) and yield strength obtained by deformation testing. It is clear from this figure that elastic wave velocity, deformation coefficient and yield strength show good mutual correlations. However, deformation coefficients have a tendency to vary slightly within the same velocity layer. This implies that deformation coefficients are apt to reflect varying conditions at different depths. Therefore, we think it is better to use elastic wave velocity in estimating overall characteristics of a formation instead of using deformation coefficient only.

Next, let us go on to the relationships between elastic wave velocity (especially S wave velocity) and other coefficients obtained from several kinds of tests. The relationship between S wave velocity and N value obtained by the standard penetration test (SPT) is shown in Figure 15. In this figure, N values obtained from testing in which the penetration cone was struck more than 50 times was extrapolated to N values for penetration of 30 cm. From Figure 15, it is clear that there is a good correlation between S wave velocity values and N values. Empirical equations expressing this relationship are given in the figure. Figure 16 shows the relationships between S wave velocity and the other elastic coefficients. Specific coefficient of soil reaction Ko and yield strength of formation Py were obtained from deformation testing using the pressure meter in a borehole. Unconfined compression strength was obtained by laboratory testing. Also, it is clear from these figures that S wave velocity has good correlations with each elastic coefficient. Empirical equations expression these relationships are given in Figure 16. Figure 17 shows a comparison of static and dynamic shear modulus. Static shear modulus was calculated from the results of borehole deformation testing. Dynamic shear modulus was calculated from elastic wave velocity and formation density. Dynamic shear modulus is larger than static shear modulus. We think that the difference between static and dynamic shear modulus may depend on differences in strain level. If the relation between stress and strain is nonlinear, the relation between static and dynamic shear modulus can be expressed as follows:

$$P = Go \cdot \varepsilon^{n} \tag{6}$$

where P is stress, ε is strain, Go is strain modulus of the apparatus at a given strain level and n is an index expression non-linearity of the formation.

Therefore, shear modulus at a given strain level is as follows:

$$G = \frac{dP}{d\varepsilon} = n \cdot Go \cdot \varepsilon^{n-1} \tag{7}$$

Because the value of n is smaller than 1, n-1 has negative values, and shear modulus G decreases according to increases in strain ε. It may be said in this connection that the strain level in PS logging is on the order of less than about 10^{-6}, while strain level in deformation testing ranges from 10^{-1} to 10^{-3}. We have at last reached the point where we can introduce our new application of PS logging; the calculation of Q value using waveform records obtained by PS logging. Q-value, which expresses the attenuation of formations, is a very important factor in calculating ground motion during earthquakes. In recent years, a variety of research on the determination of Q value has been conducted. For several years, the authors have been calculating Q value from PS logging waveforms.

The following is a familiar equation expressing the case of a wave arising from a certain point:

$$A\ (\omega,t) = Ao\ (\omega,t) \cdot r^{-a} \cdot e^{-\frac{\omega}{2QV} r} \cdot e^{-j\omega(t-r/V)} \tag{8}$$

where $A(\omega,t)$ is spectrum at the point of reception of the wave, $Ao(\omega,t)$ is spectrum at the source, ω is angular frequency, r is distance between source and receiving point, v is P and S wave velocities, Q is Q-value and a is index of geometric expansion of the wave. In equation (8), the term $e^{-j\omega,(t-r/v)}$ can be neglected because it expresses only phase shift. Also, index a is equal to 1, because, in PS logging, the source can be treated as a point source at ground surface. The P and S waves generated at the source are propagated spherically through the medium. Except for the spectrum at the source, the other quantities in Equation (8) can be obtained from the results of PS logging. Spectrum at the source $Ao(\omega)$ can be cancelled out by taking the spectral ratio between two receiving points.

However, there is one additional problem involved in the calculation of Q value, i.e., the fact that source spectra are different each time a measurement is taken. Correction for this variation is made by drilling a separate, shallow borehole adjacent to the measuring borehole. Waveform records are taken from both boreholes. Then the ratio between the two spectra obtained are calculated. If the corrected spectra at the two receiving points are designated $A_1(\omega)$ and $A_2(\omega)$, Q value can be calculated from Equation (9):

$$Q = -\frac{\omega r}{2V\left\{\ln\frac{A2\ (\omega)}{A1\ (\omega)} + \ln r\right\}} \tag{9}$$

An example of results of Q-value calculations is shown in Figure 18. In this figure, the vertical axis is distance between monitoring and receiving point and the horizontal axis is spectral ratio. Q values were calculated from many data within each velocity layer using the least square method. In this case, Q values obtained by this method corresponded closely to those obtained from in situ dynamic deformation testing, etc. Figure 19 compares Q values obtained from PS logging with those obtained from other methods. Although the data represented in the figure is insufficient, it does contain some interesting suggestions. The dynamic deformation test data was obtained in diorite. Acoustic wave data was obtained in basalt. The other data was obtained from sandstone and mudstone. The data shows that Q values are not necessarily in hard rock than in soft rock. In addition, frequency of acoustic waves was about 100 KHz, while wave frequencies in PS logging were only about 20-300 Hz. However, Q values obtained from these two methods were nearly equivalent. This suggests that Q value does not depend on frequency.

A lot of problems concerning Q value remain to be studied, e.g., whether Q value depends on strain amplitude or not. It is the authors intention to continue research on in situ Q values in different kinds of formations.

Afterword

In this paper, we have covered the measurement of elastic wave velocity and applications of this data. In particular, we have focused on S wave velocity for use in civil engineering in Japan. We conclude that S wave velocity will see more use in the future as the single most important characteristics of formations. Furthermore, S wave velocity will in the future be used to determine several characteristics of formations, such as Q value, porosity, permeability and other values.

Acknowledgements

We express the utmost gratitude to our colleagues who have helped in the development of PS logging equipment and in its use in data gathering. Also, a hearty thanks to the President of OYO Corporation, Dr. Suyama, for his guidance and many useful suggestions.

References

Haskell, N.A., 1962. Crustal Reflection of Plane SH Waves. Journal of Geophysical Research, vol. 65, pp. 4147-4150

Imai, T. and Tonouchi, K., 1982. Correlation of N Value with S-Wave Velocity and Shear Modulus. Proc. of the Second European Symposium of Penetration Testing.

Imai, T., Tonouchi, K. and Kanemori, T., 1980. Evaluation of Q Value Using S-Wave Logging Records. OYO Technical Note, No. 2, pp. 51-70.

Imai, T., 1972. P and S Wave Velocities of the Ground in Japan. Proc. of Ixth ICSMFE

Imai, T. and Yoshimura, M., 1977. The Relation of Mechanical Properties of the Soil to P and S Wave Velocities (In Japanese). Butsuri Tanko, vol. 25, No. 6

Kitsunezaki, C., 1967. Observation of S Waves by the Special Borehole Geophone (in Japanese). Butsuri Tanko, vol. 20

Kitsunezaki, C., 1980. A New method for Shear Wave Logging. Geophysics, vol. 39, No. 5. pp-1489-1506

Masuda, H., 1961. Applied Geophysical Study On the Velocity of Elastic Waves in Foundation Rock of Concrete Dams in Japan (in Japanese). CIREPI report (Civil 61006)

Ogura, K., 1979. The Development of the Suspension Type S Wave Logging System (in Japanese). OYO Technical Report, No. 1, pp 143-160.

Ogura, K. and Nakanishi, S., 1980. Development of the Suspension S Wave Logging System, Report No. 2 (in Japanese). OYO Technical Report No.2, pp. 37-50.

Shima, E. and Imai, T., 1982. The Estimation of Strong Ground Motion Due to Future Earthquakes. Proc. of 3rd Int. Earthquake Microzonation Conf. vol. 1, pp. 519-536.

Figure 1: Schematic diagram of PS logging (downhole method)

Figure 2: Example of waveform records obtained by the downhole method

Figure 3: Schematic diagram of PS logging (uphole method)

Figure 4: Example of waveform records obtained by the uphole method

Figure 5: Schematic diagram of PS logging (suspension PS logging)

Figure 6: Example of waveform records obtained by suspension PS logging

Figure 7: Example of measurement results from a soil formation. Type and location of source were changed at 40 m for both P and S waves

Figure 8: Example of measurement results for a soft rock formation. Blasting was used to generate P waves.

Figure 9: Example of measurement results for a hard rock formation. Type and location of source were changed at 46 m for P waves and 70 m for S waves, in accordance with site conditions.

Figure 10: Example of measurement result obtained by suspension PS logging

Figure 11: Example of application of S wave velocity in response analysis. This example shows results calculated for ground surface.

Figure 12: Example of application of S wave velocity in response analysis. This example shows results calculated for various depths.

Figure 13: Example of application of S wave velocity in seismic microzonation

Figure 14: Example of application of elastic wave velocity for estimation of rock characteristics. The line in the "yield strength" and "deformation coefficient" columns has no physical meaning. It is drawn to show the prominent distribution tendencies of yield strength and deformation coefficient.

Figure 15: Relationship between N value and S wave velocity

Figure 16: Relationship between several coefficients and S wave velocity

Figure 17: Relationship between static shear modulus and dynamic shear modulus

Figure 18: Example of calculation of Q value using P and S waveform records

Figure 19: Comparison of Q values obtained from PS logging and other tests

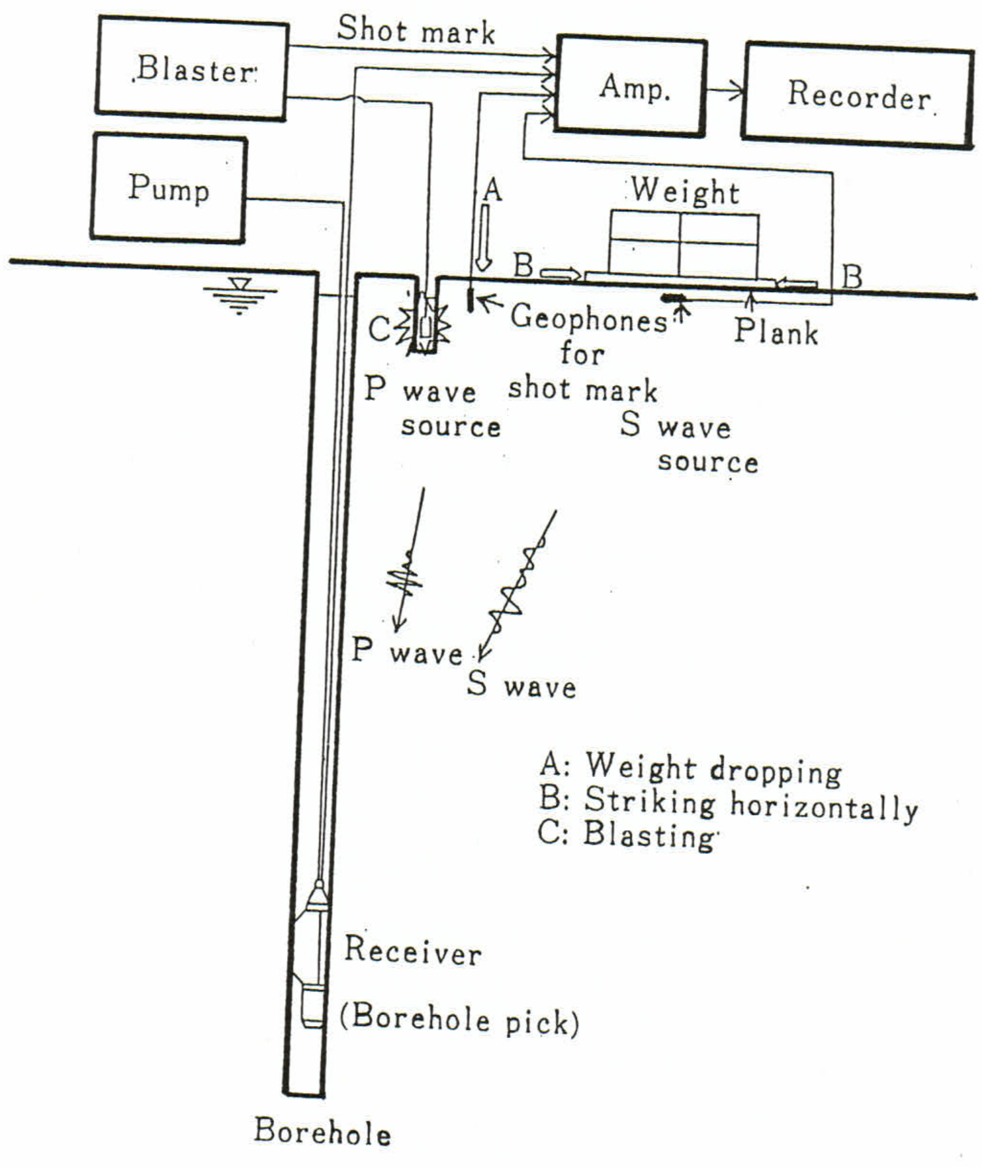

Shot mark
Blaster
Amp.
Recorder
Pump
A
Weight
B
B
C
Geophones for shot mark
Plank
P wave source
S wave source
P wave
S wave
A: Weight dropping
B: Striking horizontally
C: Blasting
Receiver
(Borehole pick)
Borehole

Fig. 1

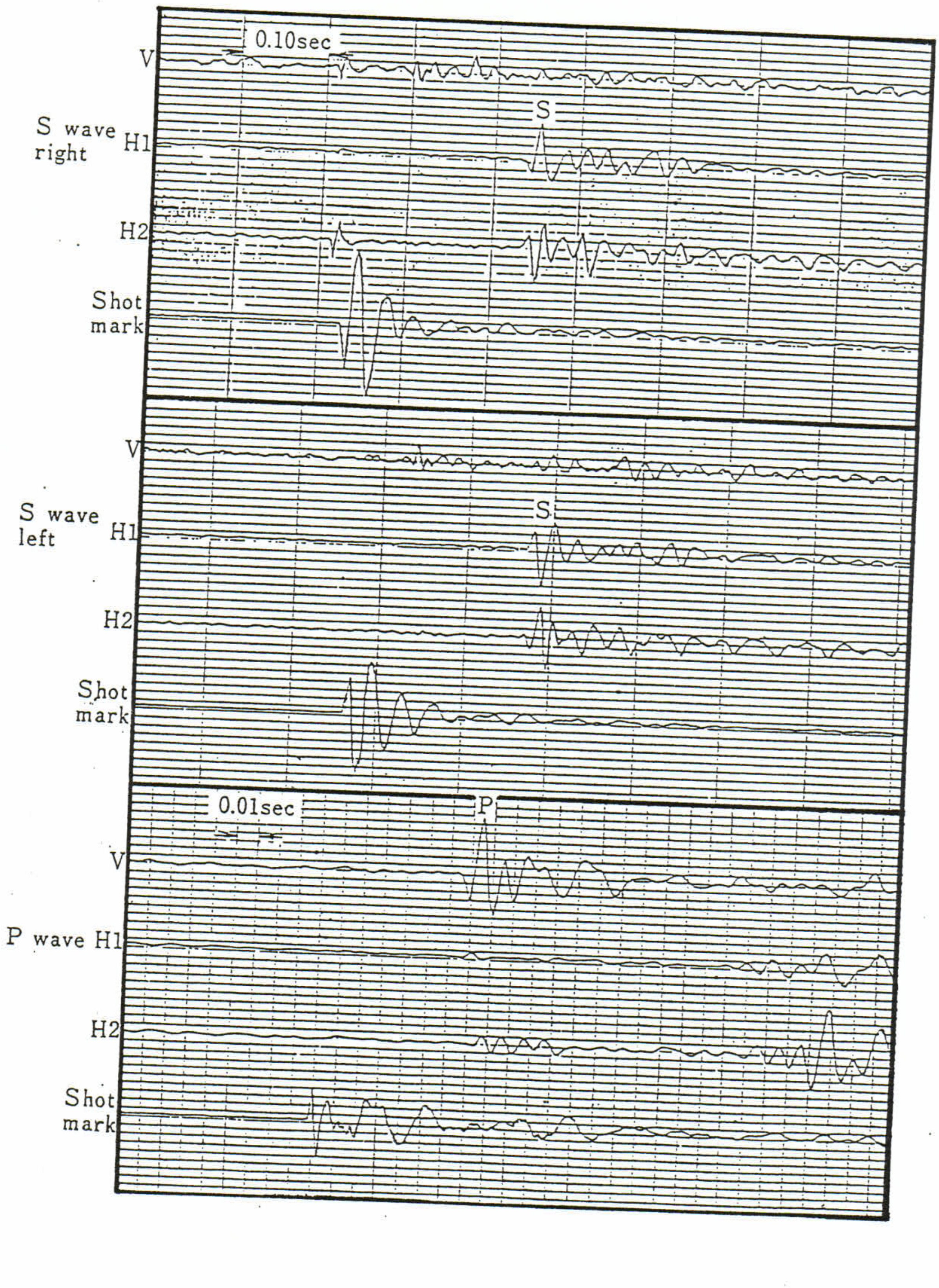
0.10sec
V
S wave right H1
S
H2
Shot mark
V
S wave left H1
S
H2
Shot mark
0.01sec
P
V
P wave H1
H2
Shot mark

Fig. 2

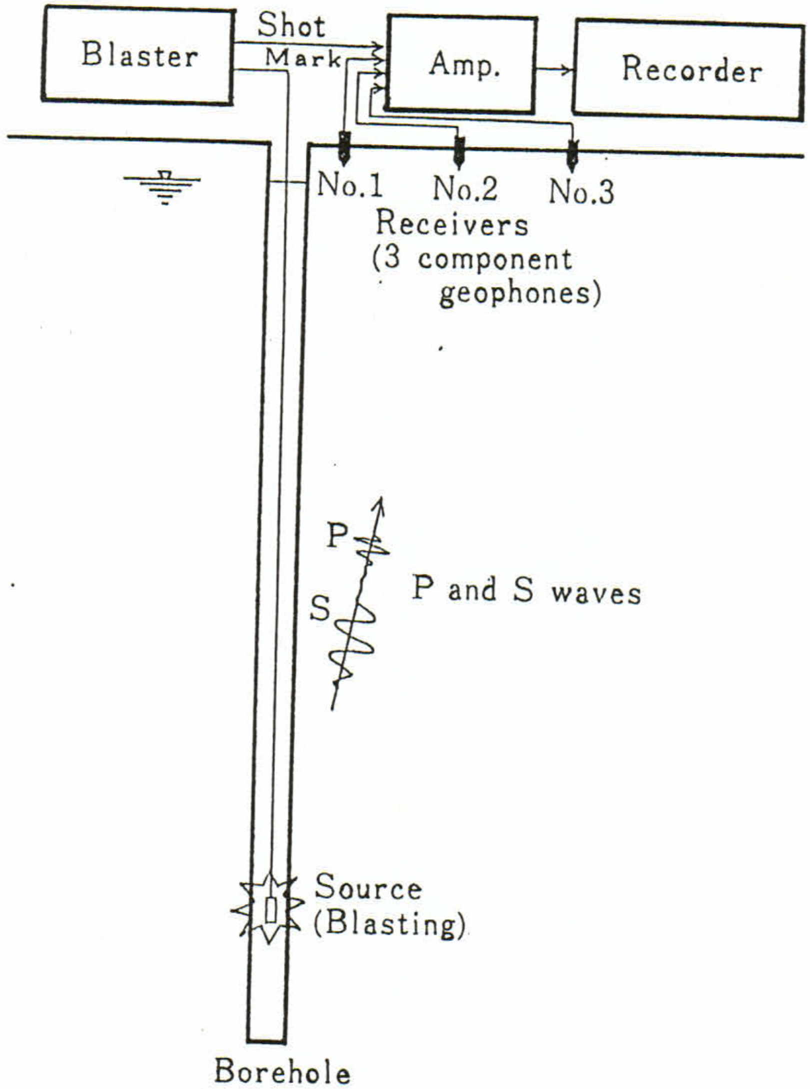
Blaster
Shot
Mark
Amp.
Recorder
No.1
No.2
No.3
Receivers
(3 component
geophones)
P
S
P and S waves
Source
(Blasting)
Borehole

Fig. 3

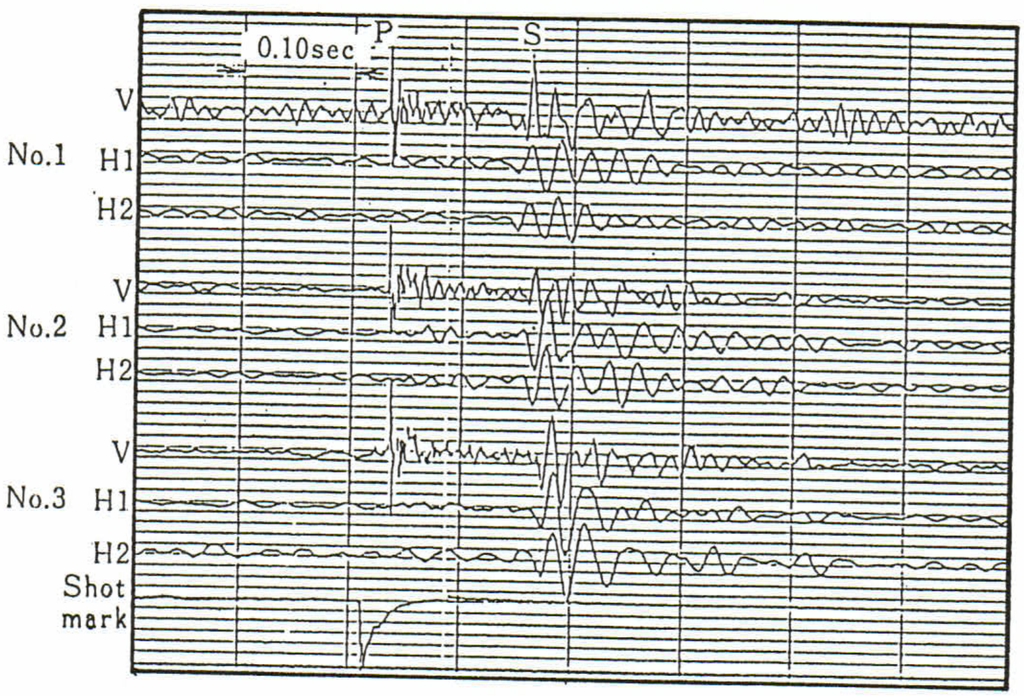

Fig. 4

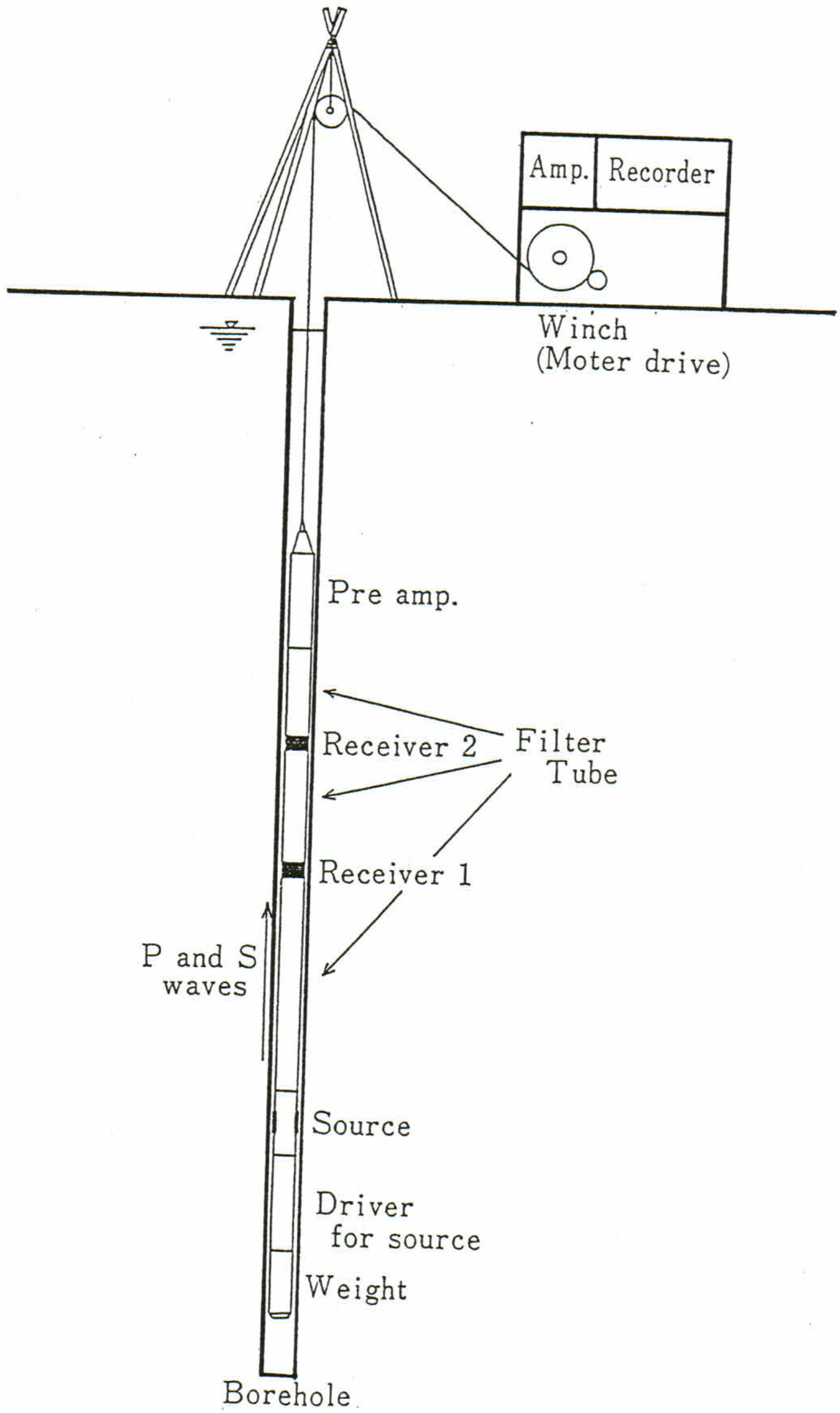
Amp.
Recorder
Winch
(Moter drive)
Pre amp.
Receiver 2
Filter
Tube
Receiver 1
P and S
waves
Source
Driver
for source
Weight
Borehole

Fig.5

FIELD: DATE:

PRE AMP: P.U.: F.T.:

DRIVER TRANSMITTER BIT DIA CASING (M)

SPACING PU1 (M) PU2 (M) T. ZERO=

DEPTH 236.0M PULSE WIDTH 1.6mSEC

DELAY 03mSEC TIME SCALE 0.4mSEC/LINE MANUAL

CH	V2	H2	H2	V1	H1	H1
GAIN	50	50	50	50	100	100
HPF(Hz)	100	100	100	100	100	100
LPF(Hz)	5 K	5 K	5 K	5 K	5 K	5 K

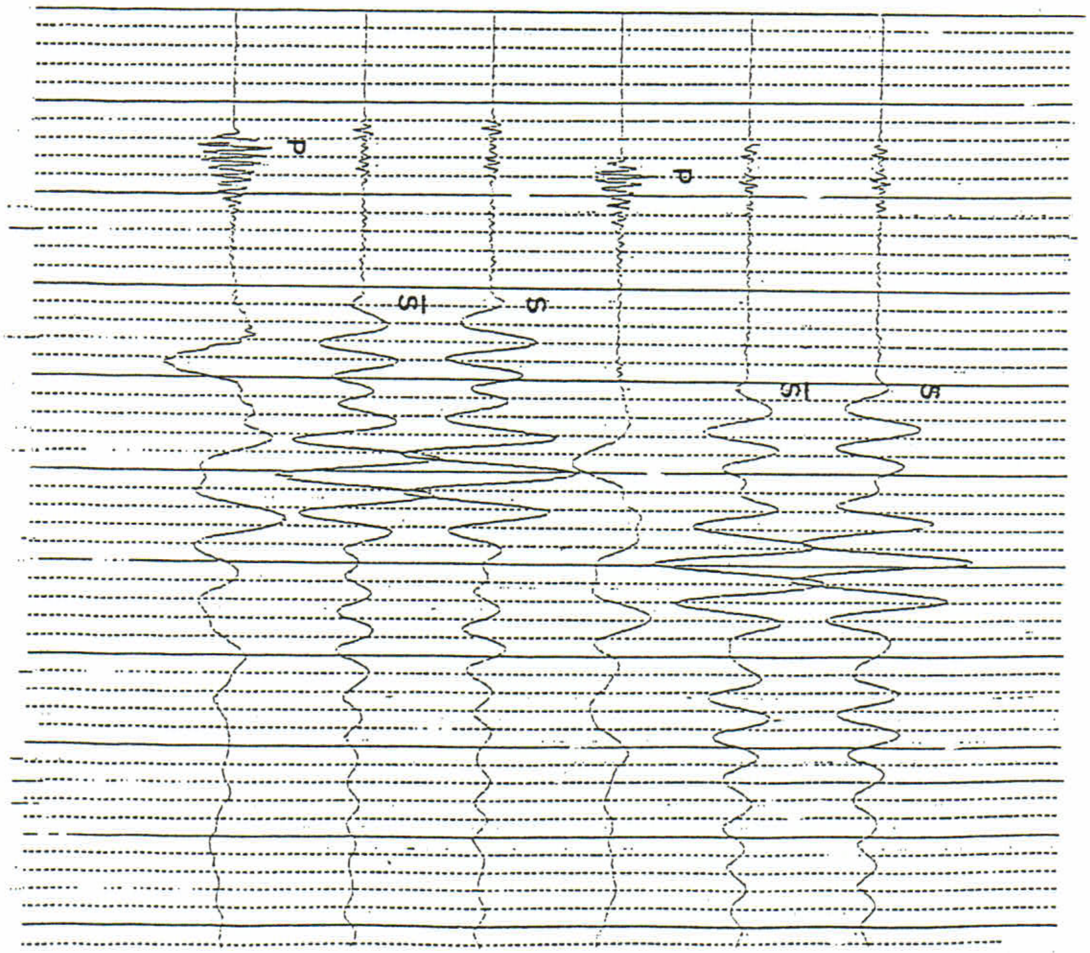

OYO SUSPENSION P-S WELL LOGS

Fig. 6

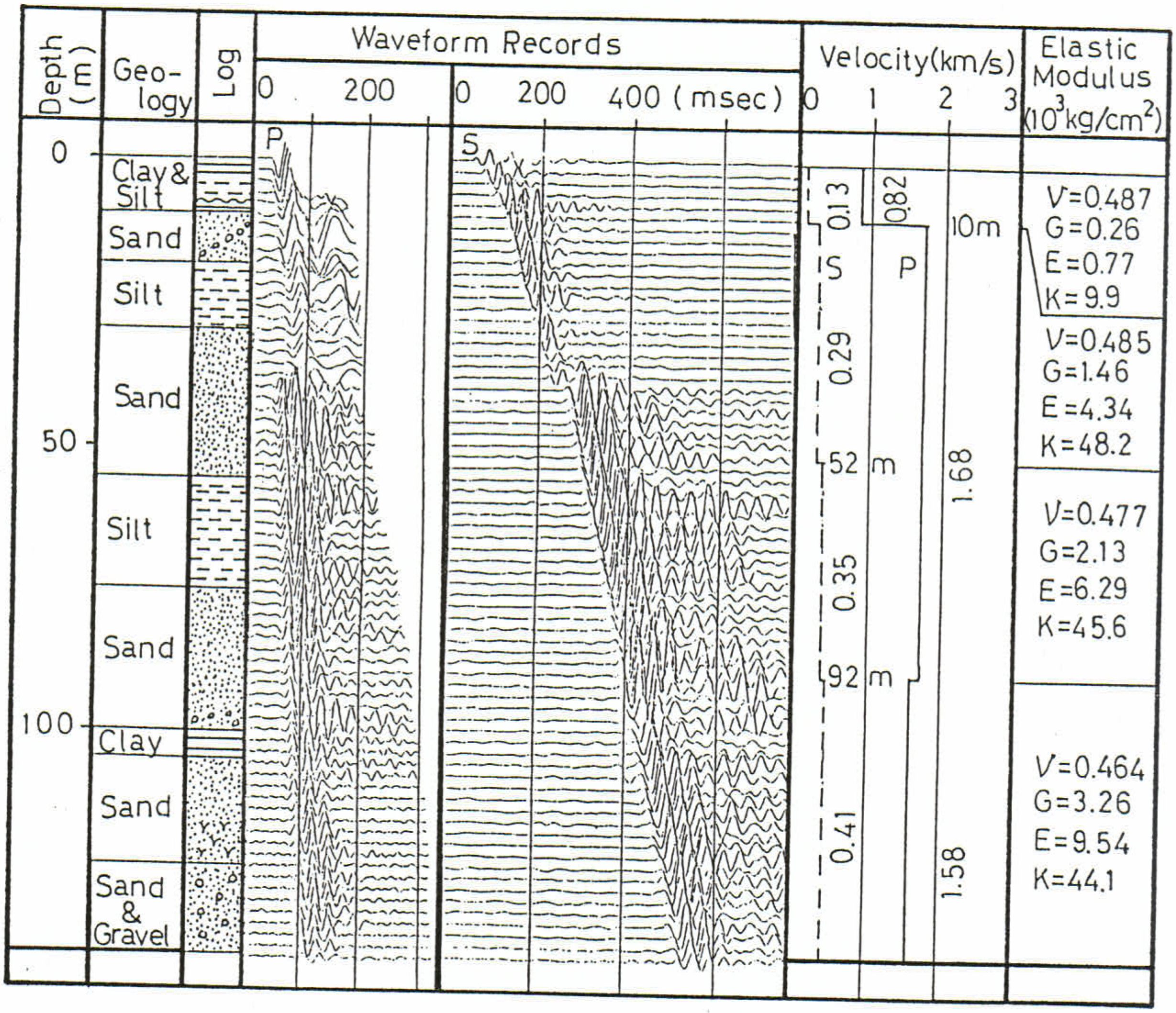

Depth (m)
Geo-logy
Log
Waveform Records
0
200
0
200
400 (msec)
Velocity(km/s)
0
1
2
3
Elastic Modulus (10^3kg/cm^2)
0
50
100
P
S
Clay & Silt
Sand
Silt
Sand
Silt
Sand
Clay
Sand
Sand & Gravel
0.13
0.82
10m
S
P
0.29
52 m
1.68
0.35
92 m
0.41
1.58
V=0.487
G=0.26
E=0.77
K=9.9
V=0.485
G=1.46
E=4.34
K=48.2
V=0.477
G=2.13
E=6.29
K=45.6
V=0.464
G=3.26
E=9.54
K=44.1

Fig. 7

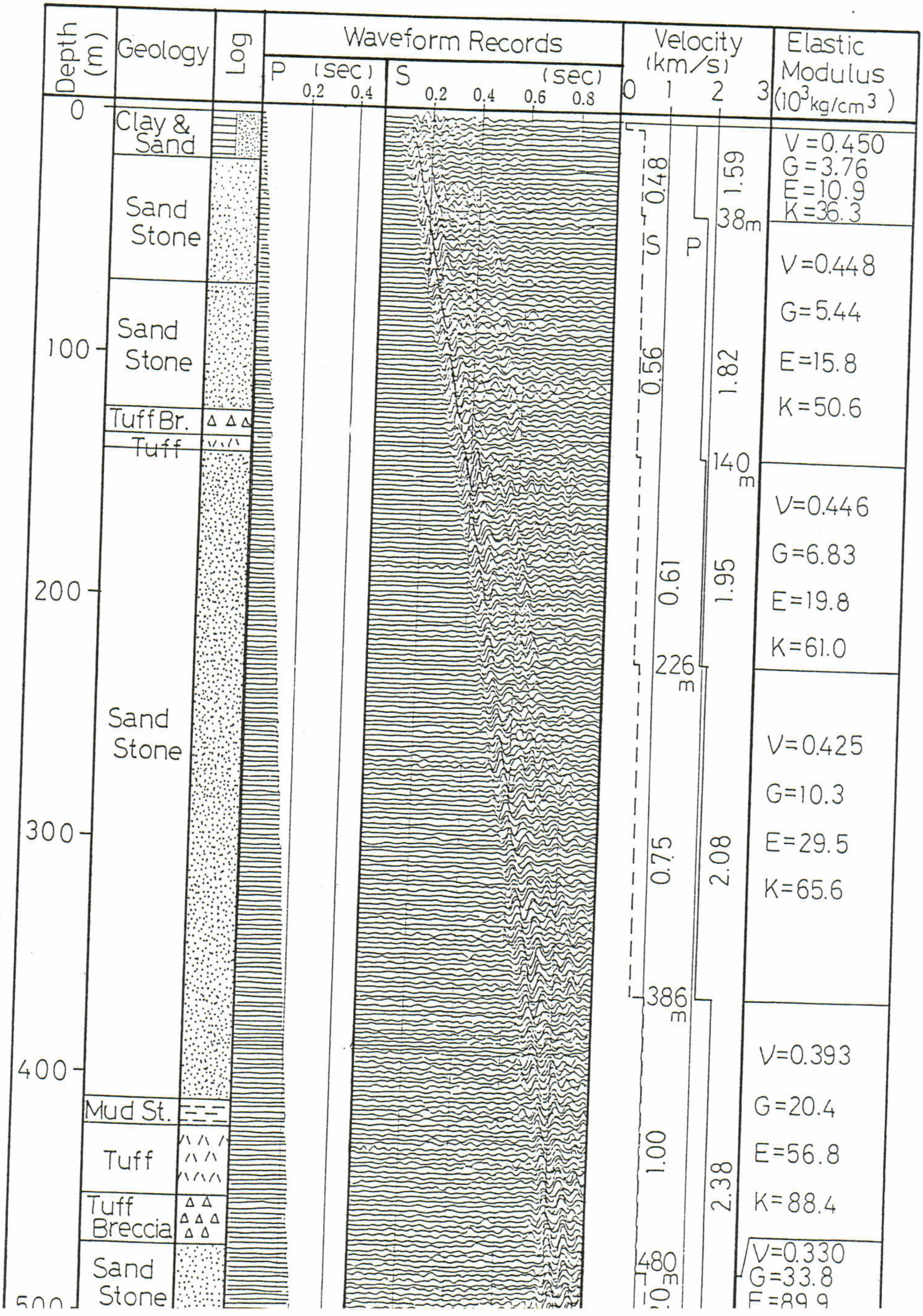
Depth (m)
Geology
Log
Waveform Records
P (sec) 0.2 0.4
S (sec) 0.2 0.4 0.6 0.8
Velocity (km/s)
0 1 2 3
Elastic Modulus (10^3 kg/cm^3)
0
100
200
300
400
500
Clay & Sand
Sand Stone
Sand Stone
Tuff Br.
Tuff
Sand Stone
Mud St.
Tuff
Tuff Breccia
Sand Stone
S
P
0.48
1.59
38m
0.56
1.82
140 m
0.61
1.95
226 m
0.75
2.08
386 m
1.00
2.38
480 m
V=0.450
G=3.76
E=10.9
K=36.3
V=0.448
G=5.44
E=15.8
K=50.6
V=0.446
G=6.83
E=19.8
K=61.0
V=0.425
G=10.3
E=29.5
K=65.6
V=0.393
G=20.4
E=56.8
K=88.4
V=0.330
G=33.8

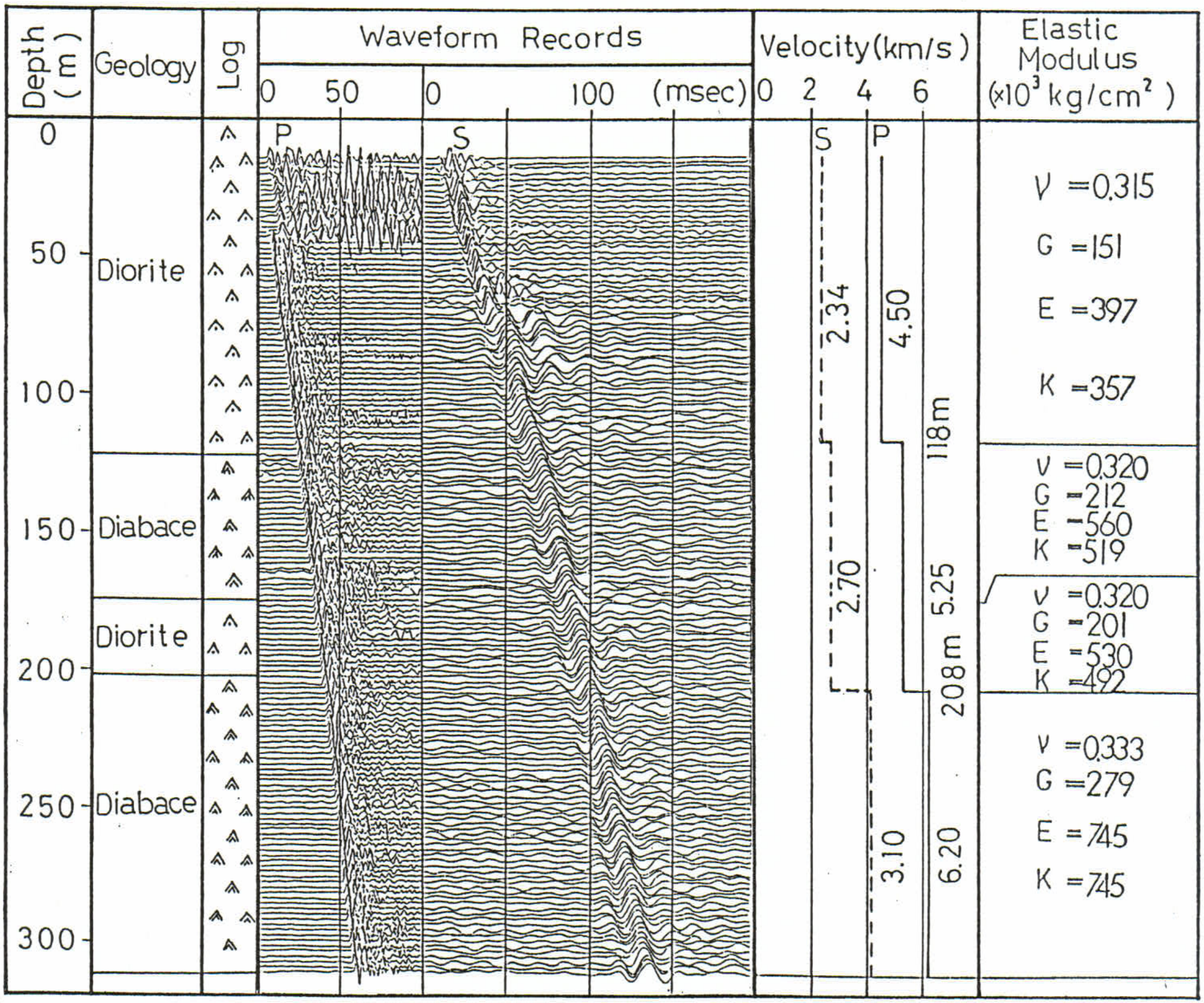
Depth (m)
Geology
Log
Waveform Records
0 50
0 100 (msec)
Velocity(km/s)
0 2 4 6
Elastic Modulus (×10³ kg/cm²)
0
50
100
150
200
250
300
Diorite
Diabace
Diorite
Diabace
P
S
S
P
2.34
4.50
118m
2.70
5.25
208m
3.10
6.20
ν =0.315
G =151
E =397
K =357
ν =0.320
G =212
E =560
K =519
ν =0.320
G =201
E =530
K =492
ν =0.333
G =279
E =745
K =745

Fig. 9

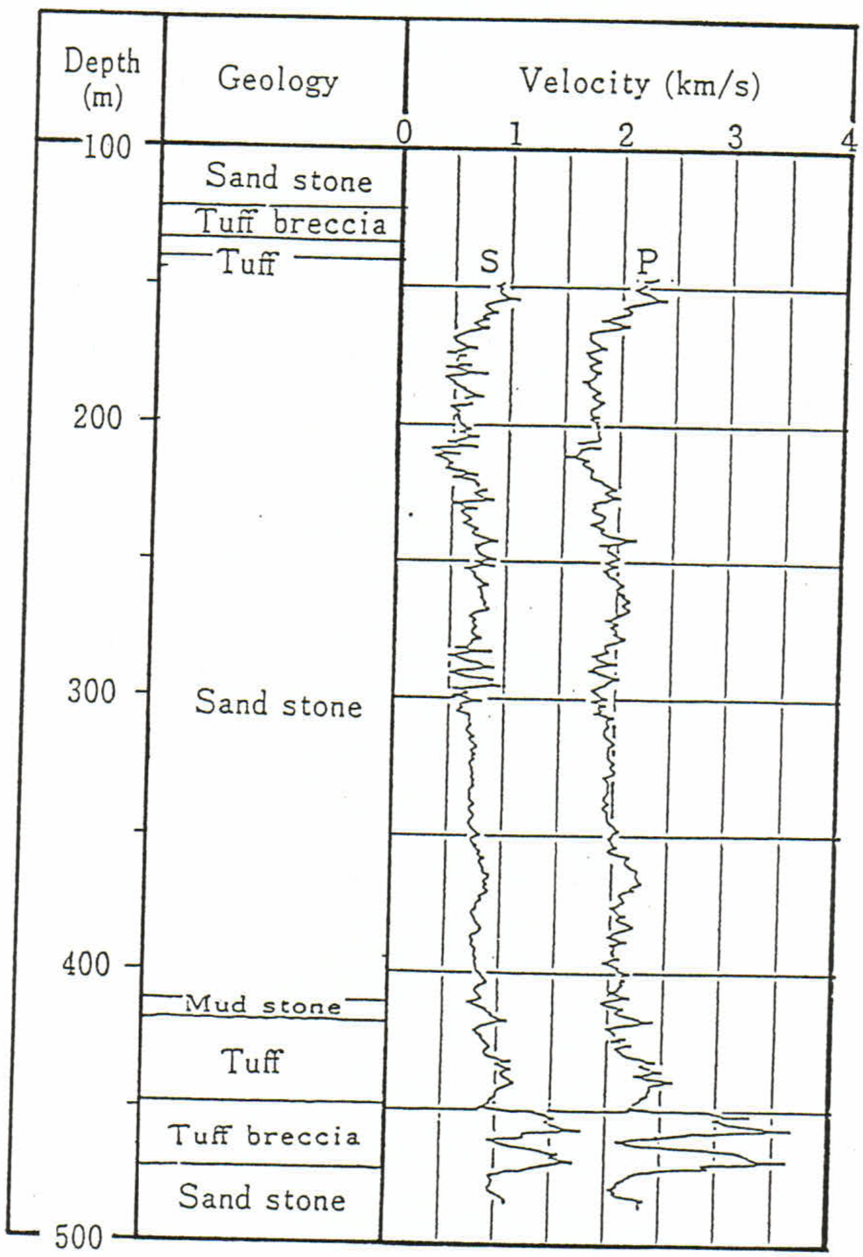

Depth (m)
Geology
Velocity (km/s)
0
1
2
3
4
100
200
300
400
500
Sand stone
Tuff breccia
Tuff
S
P
Sand stone
Mud stone
Tuff
Tuff breccia
Sand stone

Fig. 10

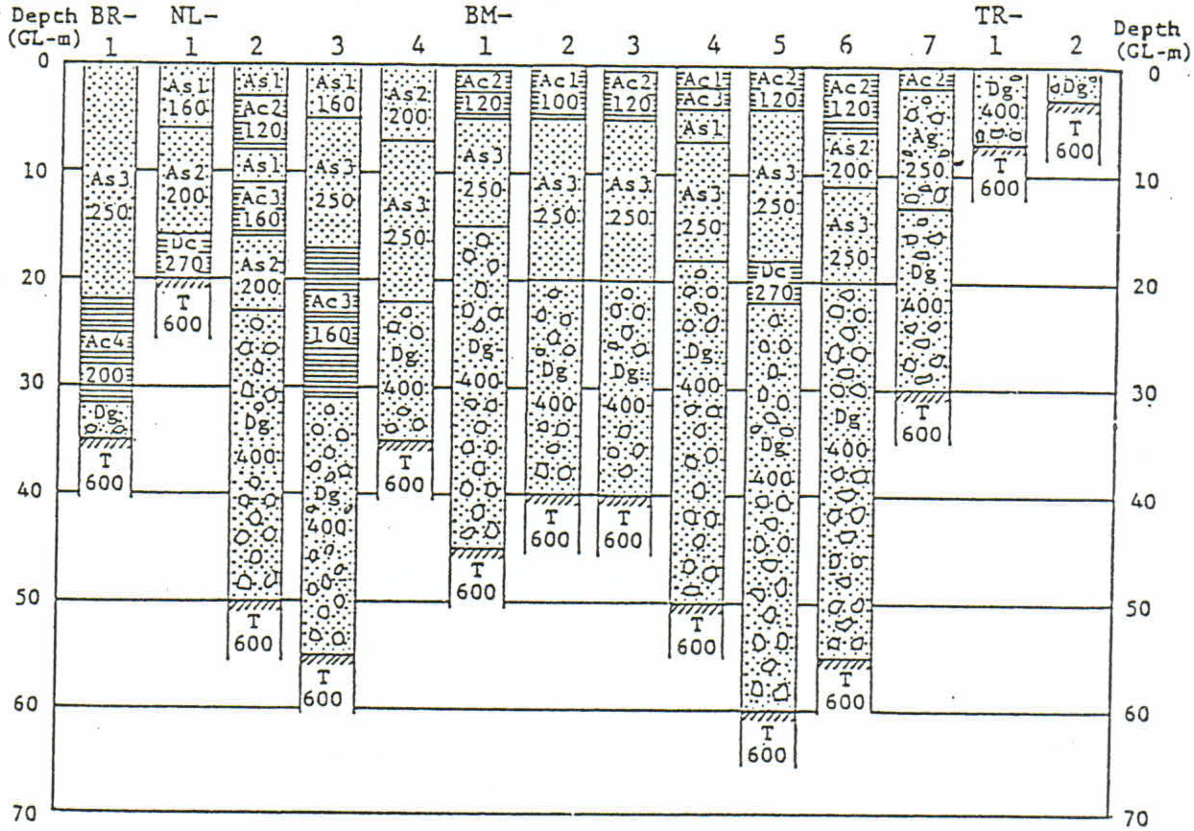

a) ground models

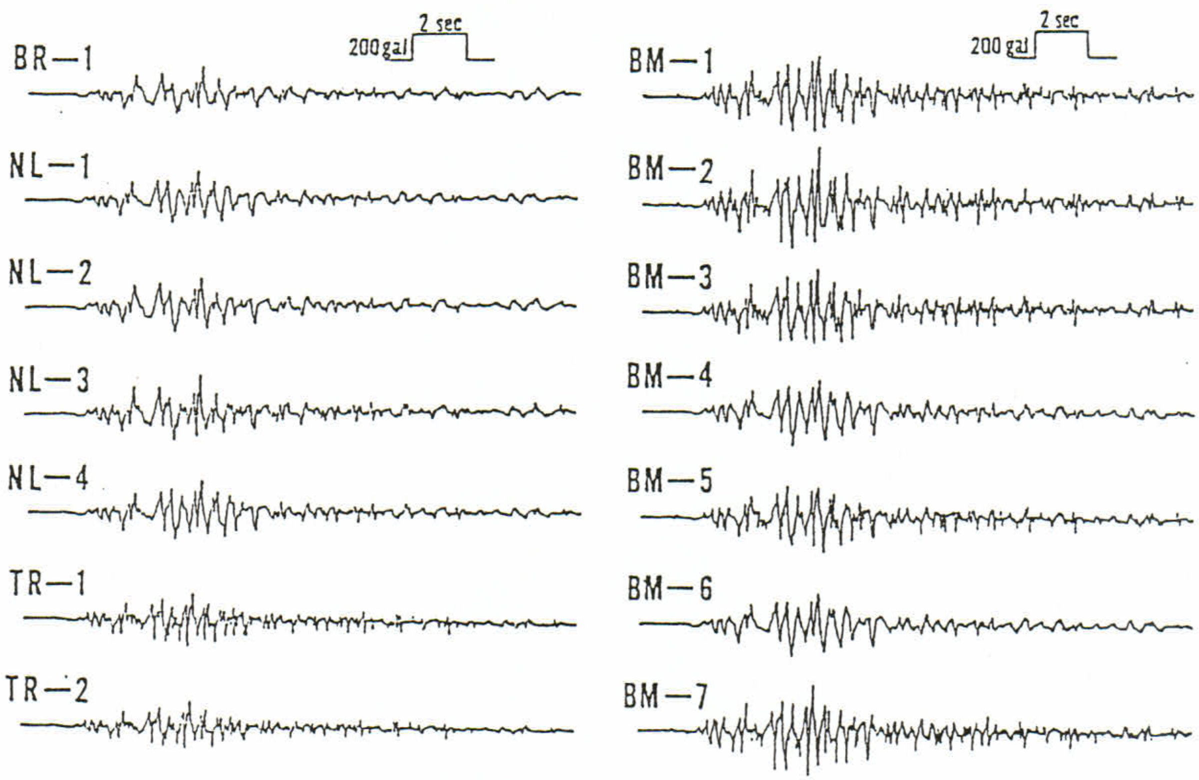

b) surface accelerograms

Fig. 11

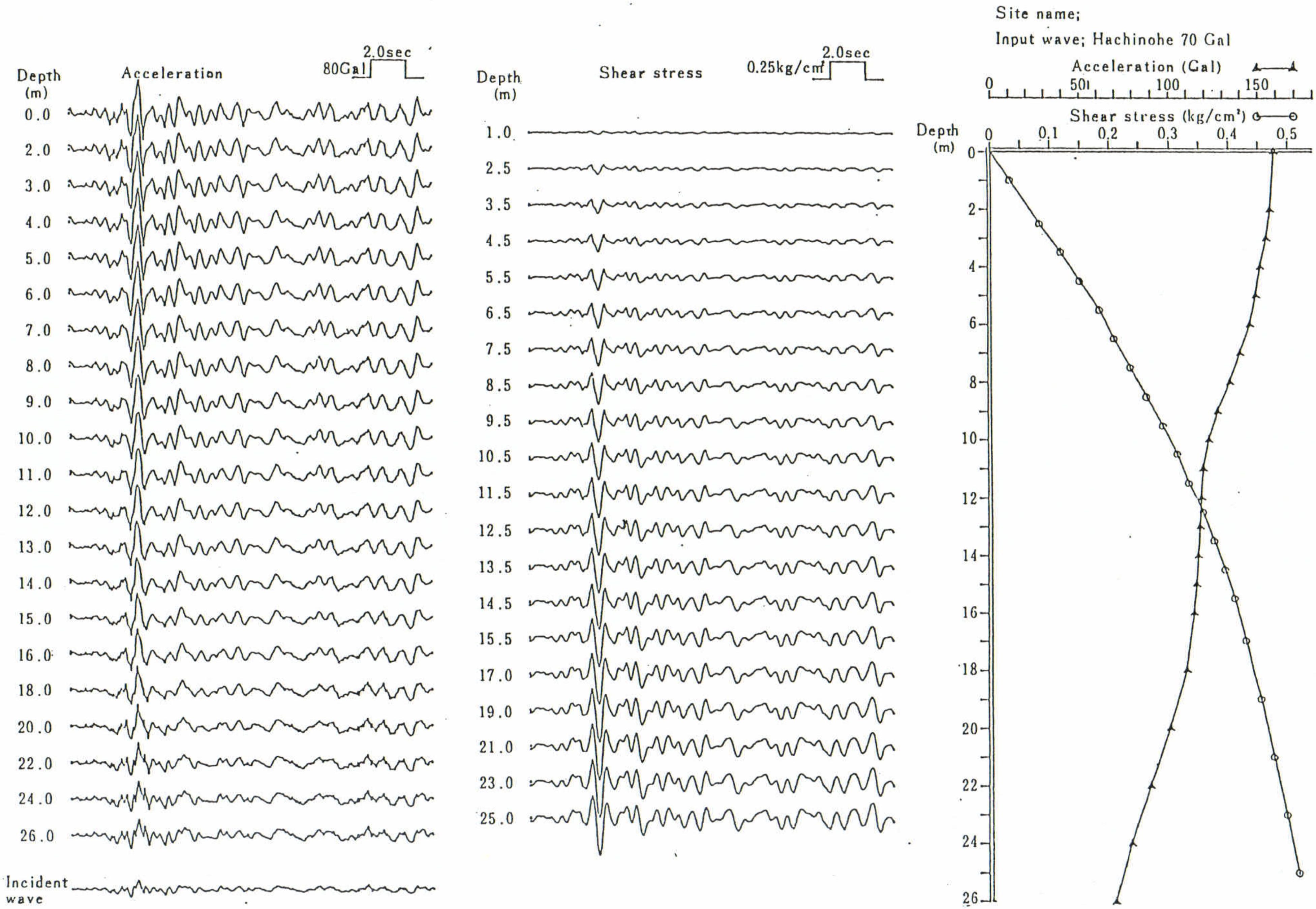
Depth (m)
Acceleration
80Gal
2.0sec
0.0
2.0
3.0
4.0
5.0
6.0
7.0
8.0
9.0
10.0
11.0
12.0
13.0
14.0
15.0
16.0
18.0
20.0
22.0
24.0
26.0
Incident wave
Depth (m)
Shear stress
0.25kg/cm²
2.0sec
1.0
2.5
3.5
4.5
5.5
6.5
7.5
8.5
9.5
10.5
11.5
12.5
13.5
14.5
15.5
17.0
19.0
21.0
23.0
25.0
Site name;
Input wave; Hachinohe 70 Gal
Acceleration (Gal)
0
50
100
150
Shear stress (kg/cm²)
0
0.1
0.2
0.3
0.4
0.5
Depth (m)
0
2
4
6
8
10
12
14
16
18
20
22
24
26

Fig. 12

Symbol	Seismic Intensity (J.M.A.)
■	Ⅶ
✳	Ⅵ +
⏻	Ⅵ −
⫲	Ⅴ +
=	Ⅴ −
+	Ⅳ +
−	Ⅳ −
•	Ⅲ

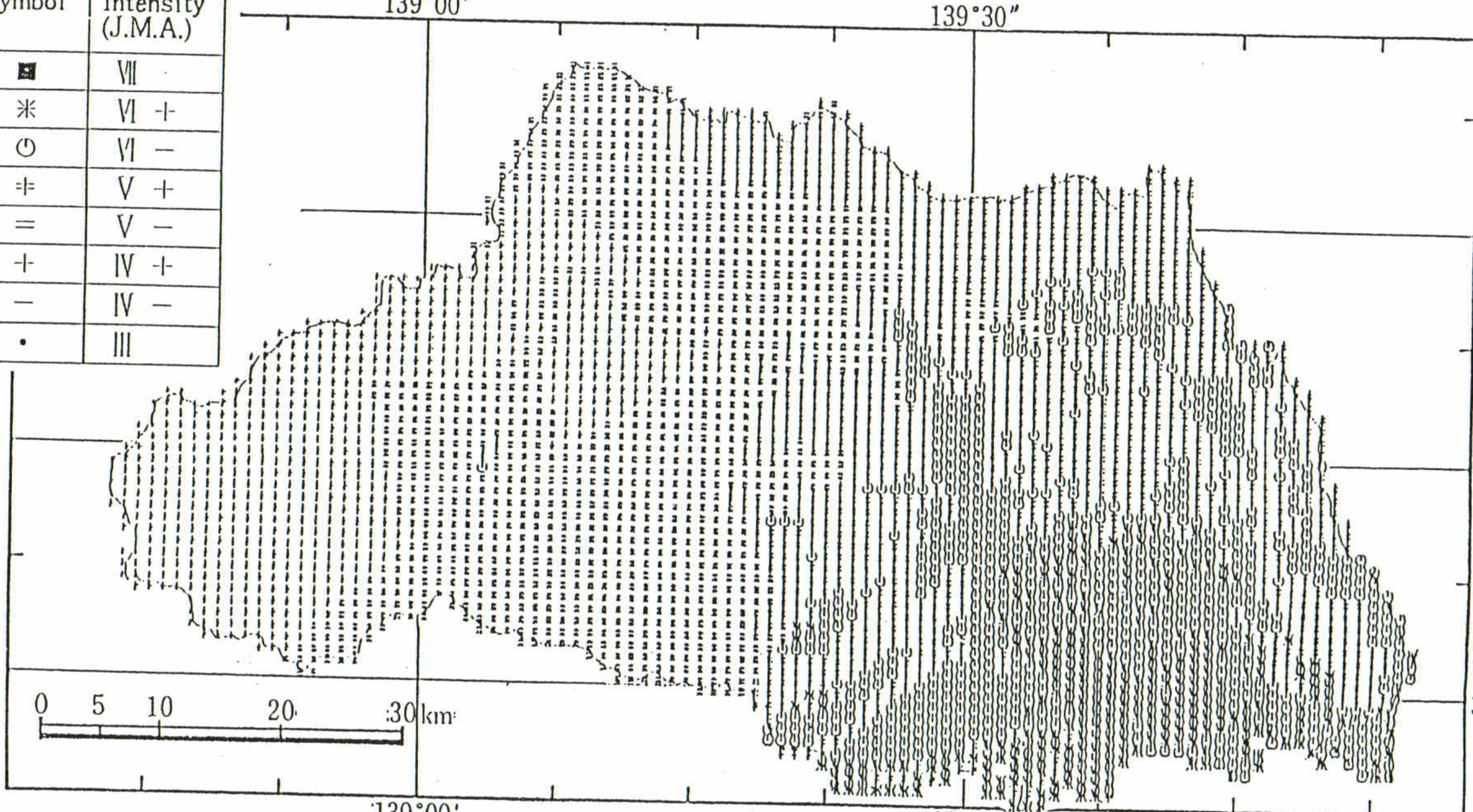

Fig. 13

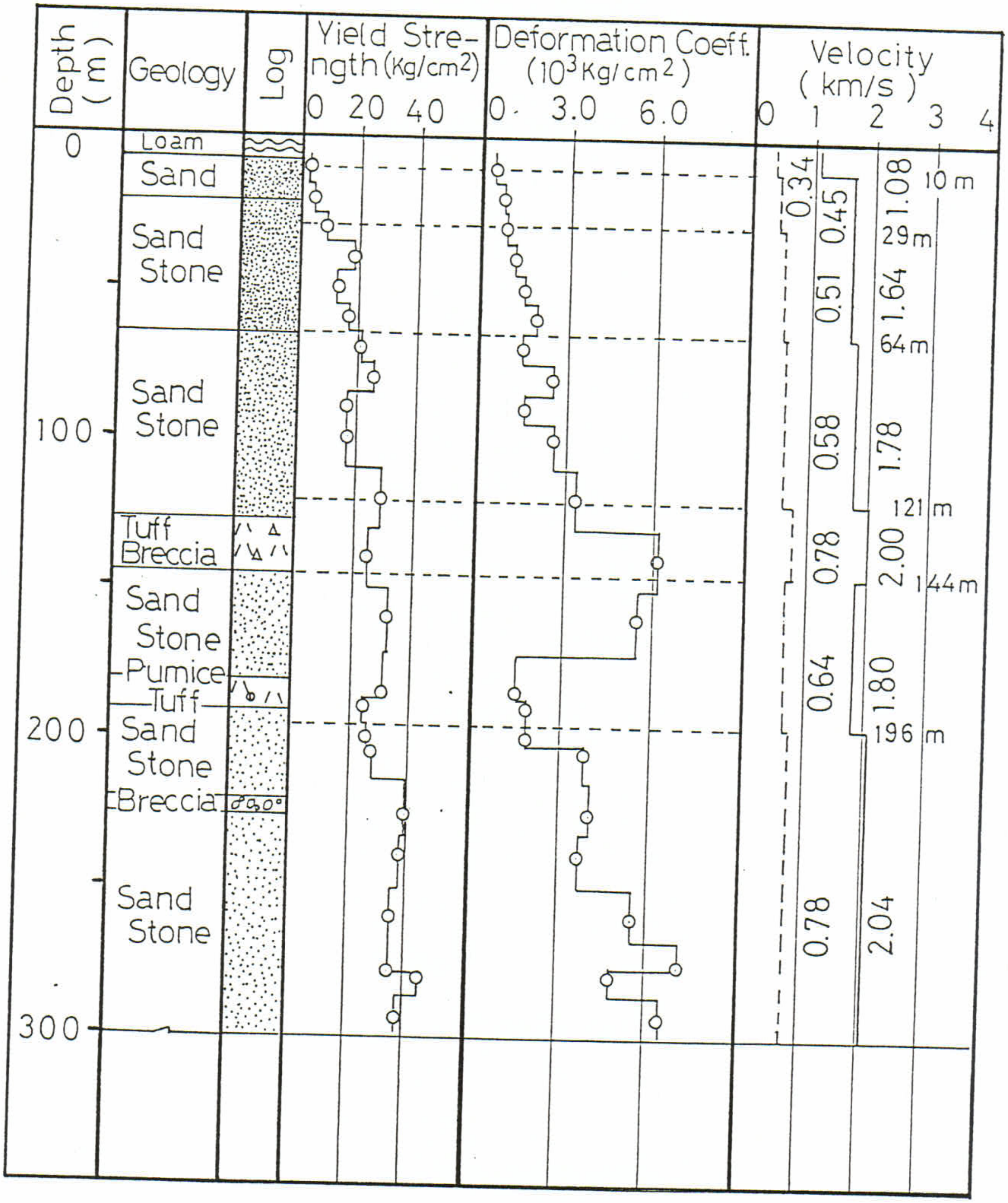

Depth (m)
Geology
Log
Yield Strength (Kg/cm2)
0 20 40
Deformation Coeff. (10³ Kg/cm²)
0 3.0 6.0
Velocity (km/s)
0 1 2 3 4
0
100
200
300
Loam
Sand
Sand Stone
Sand Stone
Tuff Breccia
Sand Stone
Pumice
Tuff
Sand Stone
Breccia
Sand Stone
0.34
0.45
0.51
0.58
0.78
0.64
0.78
1.08
1.64
1.78
2.00
1.80
2.04
10 m
29m
64m
121 m
144m
196 m

Fig. 14

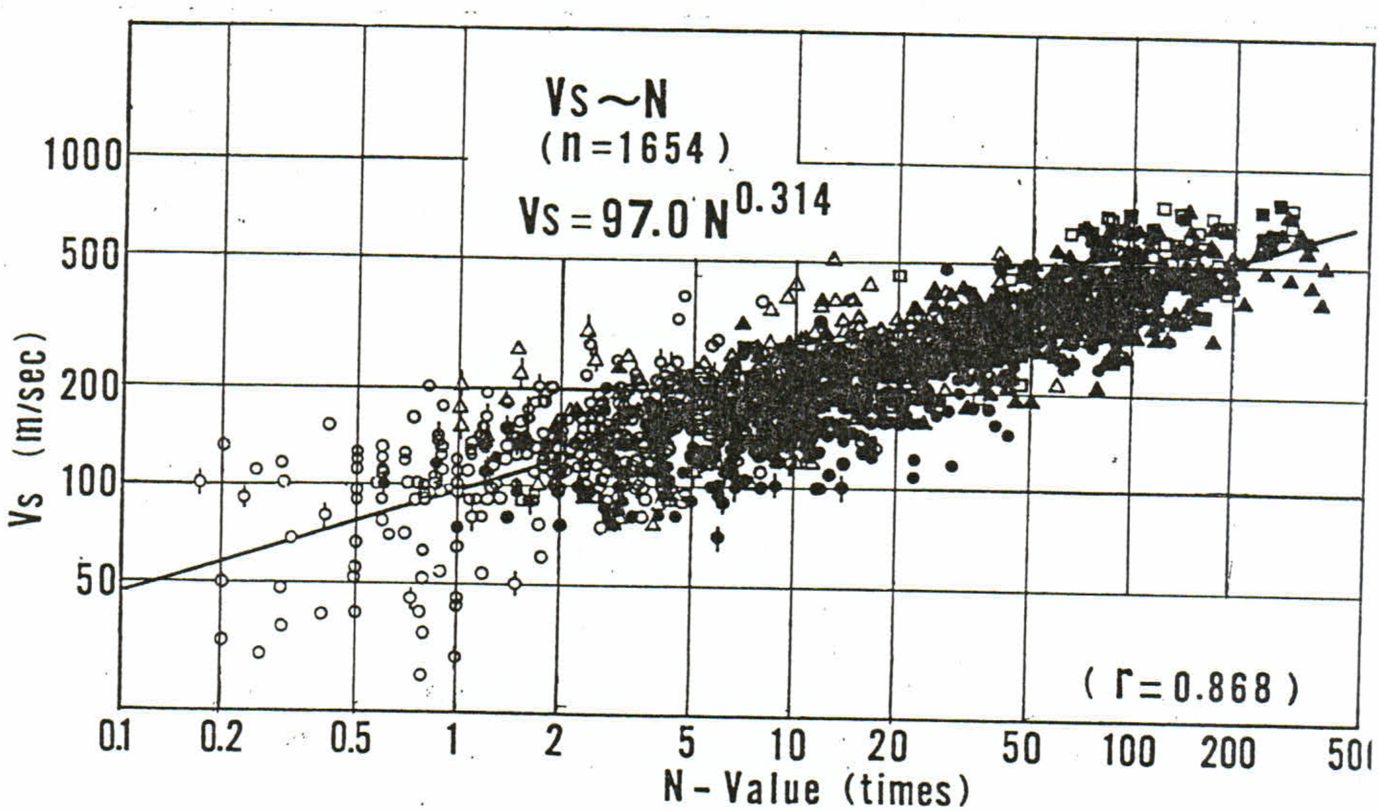
Vs ~ N
(n = 1654)
Vs = 97.0 N^0.314
1000
500
200
100
50
Vs (m/sec)
(r = 0.868)
0.1
0.2
0.5
1
2
5
10
20
50
100
200
500
N - Value (times)

Fig.15

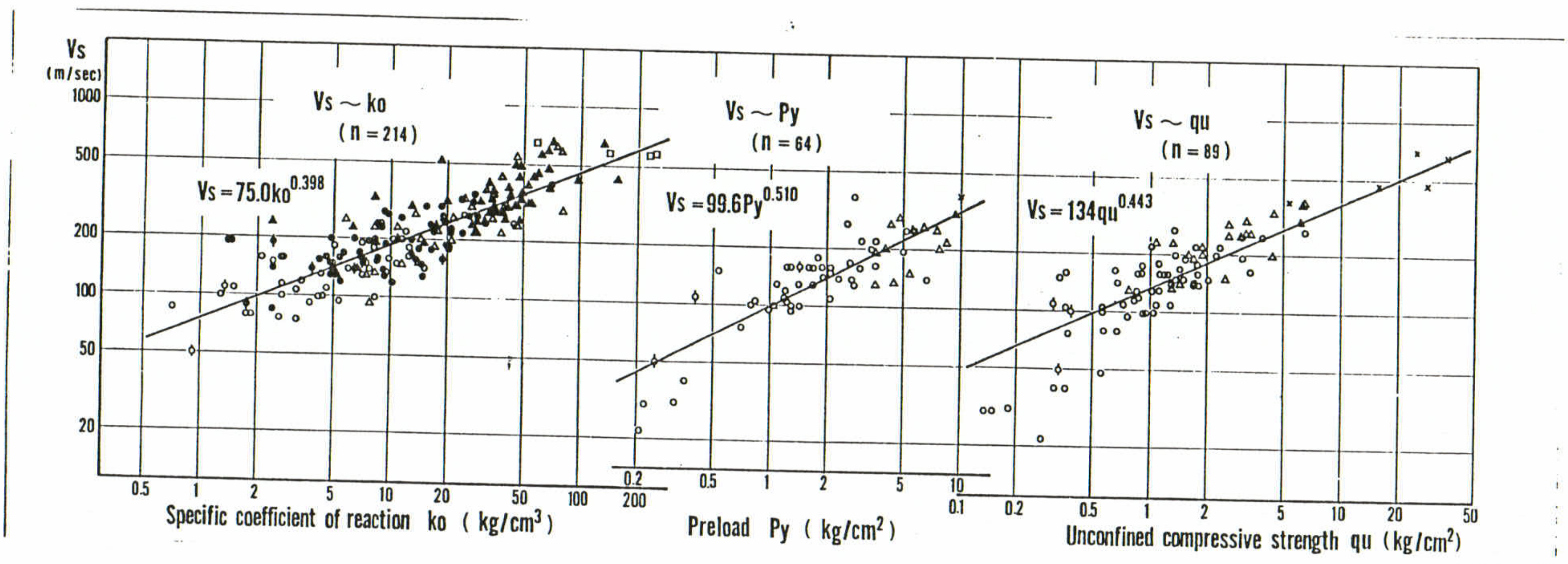
Vs (m/sec)
1000
500
200
100
50
20
Vs ~ ko
(n = 214)
Vs = 75.0ko^0.398
0.5
1
2
5
10
20
50
100
200
Specific coefficient of reaction ko (kg/cm³)
Vs ~ Py
(n = 64)
Vs = 99.6Py^0.510
0.2
0.5
1
2
5
10
Preload Py (kg/cm²)
Vs ~ qu
(n = 89)
Vs = 134qu^0.443
0.1
0.2
0.5
1
2
5
10
20
50
Unconfined compressive strength qu (kg/cm²)

Fig. 16

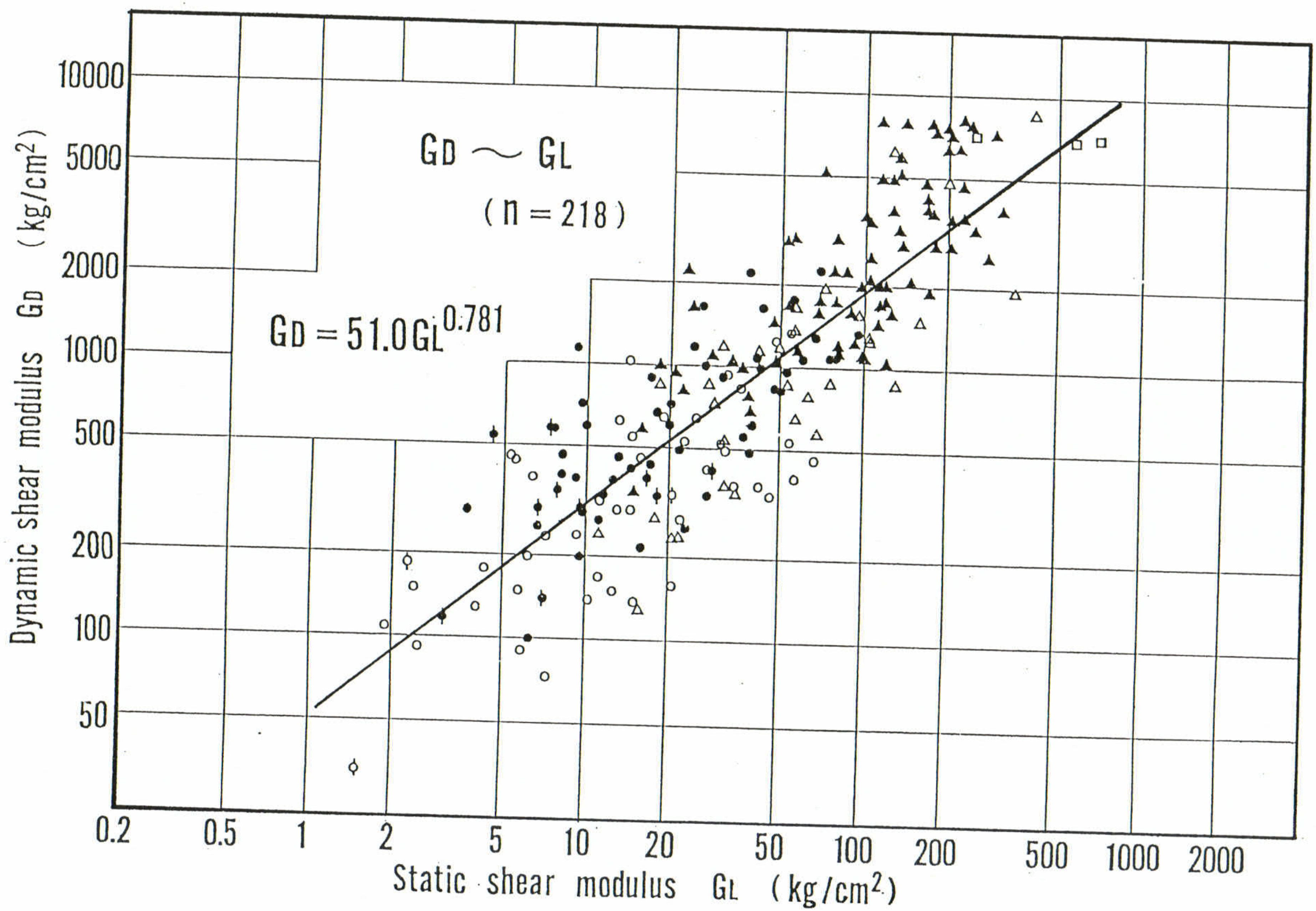

GD ~ GL
(n = 218)
GD = 51.0GL^0.781
10000
5000
2000
1000
500
200
100
50
Dynamic shear modulus GD (kg/cm2)
0.2
0.5
1
2
5
10
20
50
100
200
500
1000
2000
Static shear modulus GL (kg/cm2)

Fig. 17

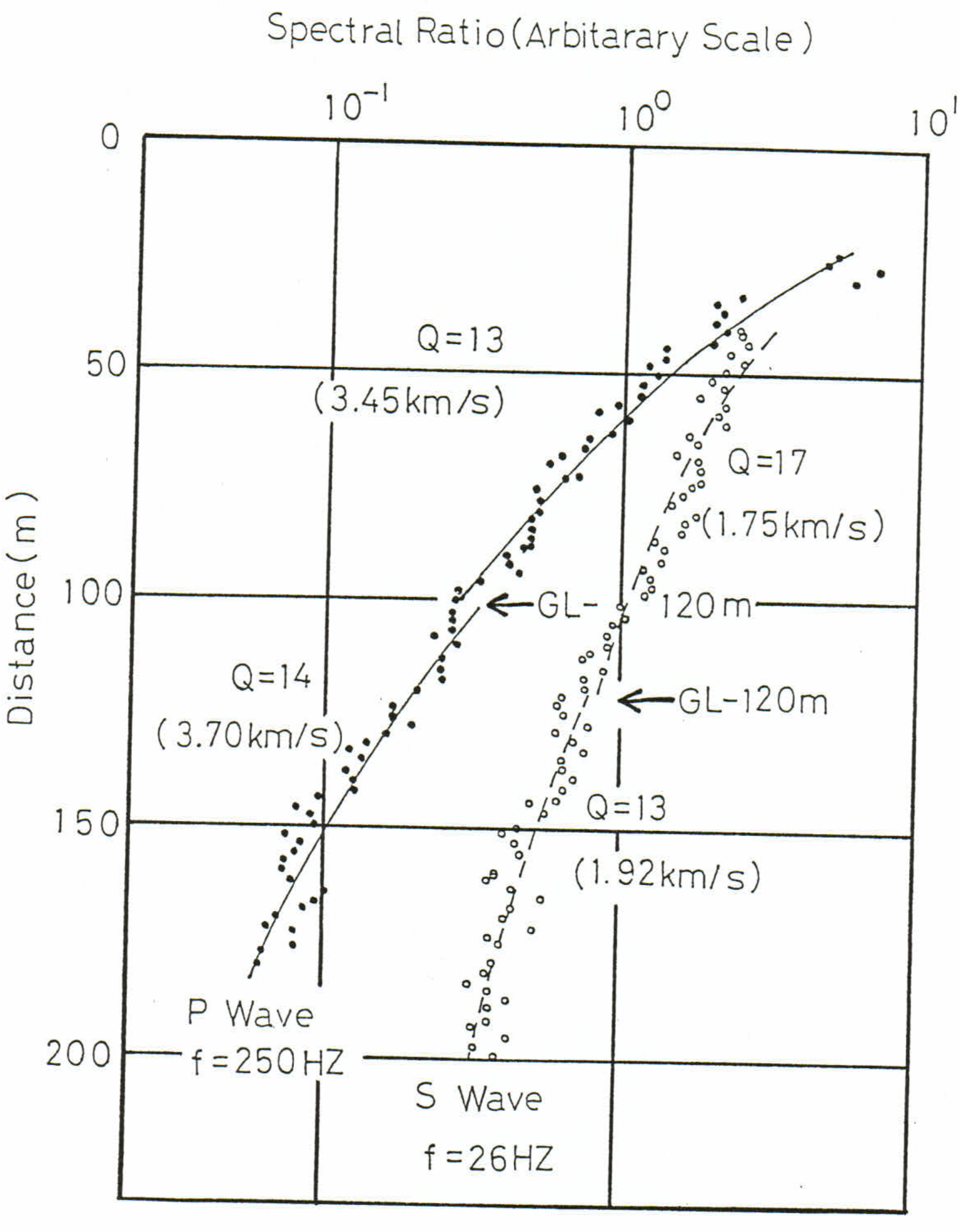
Spectral Ratio (Arbitarary Scale)
10⁻¹
10⁰
10¹
0
50
100
150
200
Distance (m)
Q=13
(3.45km/s)
Q=17
(1.75km/s)
GL-120m
GL-120m
Q=14
(3.70km/s)
Q=13
(1.92km/s)
P Wave
f=250HZ
S Wave
f=26HZ

Fig. 18

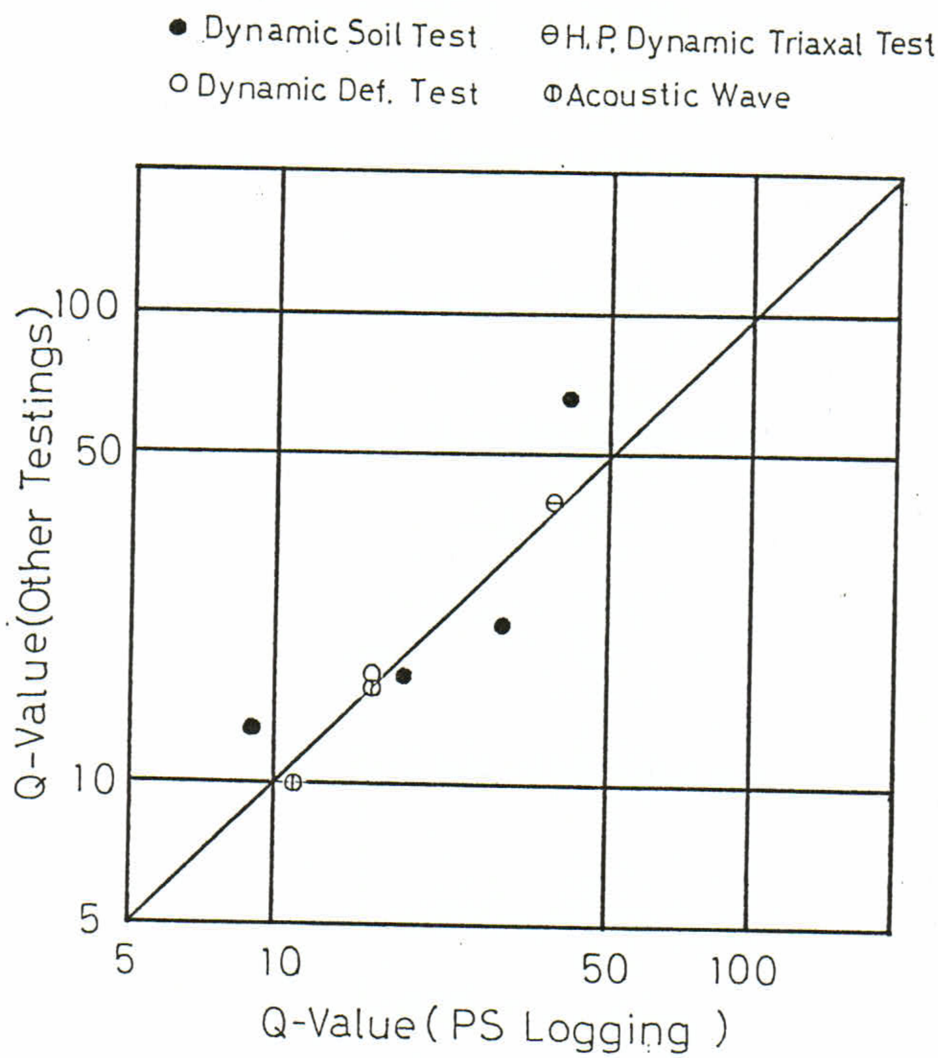
● Dynamic Soil Test
○ Dynamic Def. Test
θ H. P. Dynamic Triaxal Test
Φ Acoustic Wave
Q-Value(Other Testings)
100
50
10
5
5
10
50
100
Q-Value (PS Logging)

Fig. 19